ORGANOMETALLICS

pubs.acs.org/Organometallics Article

Improving Redox Reversibility and Intermetallic Coupling of Co(III) Alkynyls through Tuning of Frontier Orbitals

Brandon L. Mash, Yiwei Yang, and Tong Ren*



Cite This: Organometallics 2020, 39, 2019-2025



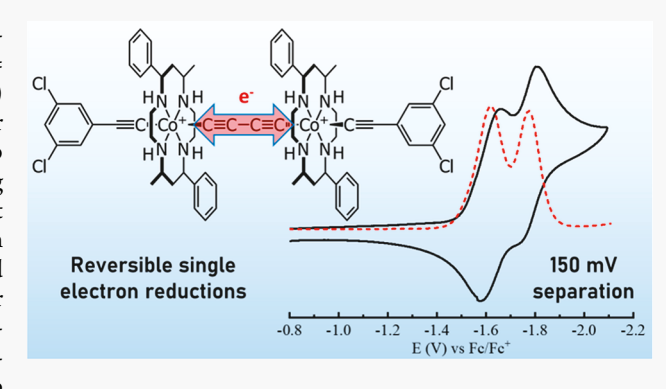
ACCESS

Metrics & More

Article Recommendations

s Supporting Information

ABSTRACT: Reported herein are the syntheses and characterizations for a series of butadiyndiyl-bridged $Co^{III}(MPC)$ (MPC = 5,12-dimethyl-7,14-diphenyl-1,4,8,11-tetraazacyclotetradecane) complexes, capped with chloride ([1]²⁺), phenylacetylide ([2]²⁺), or 3,5-dichlorophenylacetylide ([3]²⁺). The MPC ligand was chosen to weaken the ligand field around the equatorial plane, allowing stronger axial coordination. Cyclic voltammetry measurement revealed the first unambiguous examples of stepwise one-electron reductions in bridged Co(cyclam') complexes (cyclam' = any ligand bearing the 1,4,8,11-tetraazacyclotetradecane framework). Further voltammetric analysis using NBu_4BArF (NBu_4BArF = tetrabuty-lammonium tetrakis[3,5-bis(trifluoromethyl)phenyl]borate) as electrolyte resulted in well-separated reversible reduction waves with up



to 160 mV separation for $[2]^{2+}$. These features hint at the possibility of application of earth-abundant metal complexes to function as molecular wires. These complexes were also characterized with infrared and UV-vis spectroscopy, density functional theory calculations, and single-crystal X-ray diffraction ($[1](BPh_4)_2$ only).

INTRODUCTION

Following the seminal work on organometallic σ -alkynyl complexes by Nast and co-workers, ^{1,2} considerable attention has been given to the application of these compounds as electronic and optoelectronic materials due to their structural rigidity and high degree of conjugation. ^{3–6} In particular, the use of metal alkynyls as the prototypical molecular wires has been investigated by the laboratories of Launay, ^{7,8} Gladysz, ^{9,10} Halet, ^{11,12} Rigaut, ¹³ and Akita. ¹⁴ Compounds exhibiting extraordinary degrees of electron delocalization include those of Fe, ¹⁵ Mn, ¹⁶ Ru, ¹⁷ Ru₂, ^{18–20} and Re. ^{21,22} Though rare, single-molecule conductance has been measured for alkynyl compounds of Pt, ^{23,24} Ru, ^{25–27} and Ru₂, ^{28,29} and functional devices have been fabricated as well. ^{30–33}

With the desire to use more earth-abundant elements and cost-efficient resources, our recent efforts have focused on cyclam complexes of 3d transition metals (cyclam = 1,4,8,11-tetraazacyclotetradecane). Our work, ^{34,35} along with those from the laboratories of Shores, ^{36,37} Nishijo, ^{38–42} and Wagenknecht, ^{43–48} has significantly expanded the scope of this previously underexplored field. While previous work on dicobalt species bridged by oligoynes revealed the structural features similar to highly delocalized Ru₂ compounds, their voltammetric responses were not ideal. The dicobalt species typically displays irreversible two-electron reductions, indicating localized charges on each cobalt center and chemical instability upon reduction, ^{49–51} the latter of which is associated

with the lability of the axial chloro-/alkynyl ligands upon the reduction of $\mathrm{Co}^{\mathrm{III}}$ center.

Reversible reduction of $Co^{III}(cyclam)$ complexes has been achieved thus far only through the use of significantly electron-withdrawing axial ligands, which are less labile on the reduced Co^{II} center. A3,46,48,52 Recently, we reported that a Co^{III} complex of a C-substituted cylam, $[Co(MPC)(C_2Ph)_2]^+$ $(MPC = 5,12\text{-dimethyl-7,14-diphenyl-1,4,8,11-tetrazazacyclote-tradecane)$, displays a quasi-reversible reduction, a in stark contrast to the irreversible reduction displayed by $[Co(cyclam)(C_2Ph)_2]^+$. Similar in effect to the use of electron-withdrawing ligands, this change in voltammetric behavior is achieved through the strengthening of the axial bonds, which is the result of a weakened equatorial ligand field. Addition of bulky phenyl groups to the cyclam skeleton appears to stiffen the macrocyle, which results in significantly weakened Co-N bonds and a net increase in positive charge density on the metal, thereby allowing stronger $Co-\sigma$ -alkynyl bonds.

It is the goal of the present work to determine if the increased electrochemical stability and axial ligand bond

Received: March 17, 2020 Published: April 28, 2020





strength of $\text{Co}^{\text{III}}(\text{MPC})$ complexes translate into discernible electronic coupling between two cobalt centers bridged by an oligoyne. To this end, a series of butadiyndiyl-bridged complexes, $[\{\text{Co}(\text{MPC})\text{Cl}\}_2(\mu\text{-C}_4)]\text{Cl}_2$ ($[\mathbf{1}]\text{Cl}_2$), $[\{\text{Co}(\text{MPC})(\text{C}_2\text{Ph})\}_2(\mu\text{-C}_4)]\text{Cl}_2$ ($[\mathbf{2}]\text{Cl}_2$), and $[\{\text{Co}(\text{MPC})(\text{C}_2\text{-3},5\text{-Cl-C}_6\text{H}_3)\}_2(\mu\text{-C}_4)]\text{Cl}_2$ ($[\mathbf{3}]\text{Cl}_2$), have been prepared (Chart 1). The syntheses and characterizations of $[\mathbf{1}]^{2+}$ – $[\mathbf{3}]^{2+}$ will be discussed henceforth.

Chart 1. Structures of Complexes [1]Cl₂-[3]Cl₂

$$2CI^{-} \qquad [1]CI_{2}: X = CI$$

$$X \left(\begin{array}{c} CO^{+} \\ \end{array} \right) C = C - C = C \\ \begin{array}{c} CO^{+} \\ \end{array} \right) X = C = C$$

$$[3]CI_{2}: X = C = C$$

$$[3]CI_{2}: X = C = C = C = C$$

■ RESULTS AND DISCUSSION

Synthesis. [Co(MPC)Cl₂]Cl and 0.5 equiv of 1,4-bis-(trimethylsilyl)butadiyne were refluxed in MeOH and Et₃N for 24 h under N₂₁ and the crude product from the reaction was purified on silica gel and recrystallized to afford [{Co(MPC)- $Cl_{2}(\mu-C_{4})Cl_{2}$ ([1]Cl₂) in 44% yield with [Co(MPC)Cl₂]Cl and [Co(MPC)(C₄H)Cl]Cl as the major byproducts. Increased reaction time did not significantly increase the ratio of product to starting material. The reactions between $[\{Co(MPC)Cl\}_2(\mu-C_4)]Cl_2$ and excess LiC_2Ar (prepared from lithium diisopropylamide) at -78 °C, using standard Schlenk techniques under nitrogen atmosphere, resulted in near quantitative conversion to $[\{Co(MPC)(C_2Ar)\}_2(\mu-C_4)]Cl_2$ with minimal scrambling of acetylides or undesired products (Scheme 1). When alkynylation of [1]Cl₂ is performed at room temperature, various mononuclear and dinuclear alkynyl products of various combinations form, as determined by mass spectrometry, and were not isolated or further characterized. Compounds [2]Cl₂ and [3]Cl₂ were isolated in 68 and 52% yields (based on [1]Cl₂), respectively.

Typical for strong-field Co(III) species, complexes [1]Cl₂, [2]Cl₂, and [3]Cl₂ are diamagnetic and exhibit well behaved ¹H NMR spectra (Figures S6–S8). The UV–vis spectra featured the d–d bands at 520 nm for [1]Cl₂, 484 nm for

[2]Cl₂, and 479 nm for [3]Cl₂, and intense LMCT ([1]Cl₂–[3]Cl₂) and π – π * ([2]Cl₂ and [3]Cl₂) bands in the UV region (Figure S10). In spite of the Co–Co coupling detected in the voltammetric study (see below), there is no significant feature associated with intermetallic coupling in the absorption spectra. The IR peaks between 2000–2100 cm⁻¹, the window for ν (C \equiv C), were barely discernible for [1]Cl₂ because of the centro-symmetric nature of the butydiynyl bridge, but fairly intense for [2]Cl₂ and [3]Cl₂ because of the contribution from the capping aryl acetylides (Figure S11).

Molecular Structures. While X-ray quality single crystals of [1]Cl₂ could not be obtained, single crystals of [1](BPh₄)₂ were successfully grown. Suitable crystals for $[2]^{2+}$ and $[3]^{2+}$ could not be obtained despite many attempts with different counterions and solvent combinations. The ORTEP plot for [1](BPh₄)₂ is given in Figure 1, while additional experimental

Figure 1. Molecular structure of $[1]^{2+}$ at 30% probability level. Hydrogen atoms and tetraphenylborate anions have been removed for clarity.

and refinement details are given in Table S1. As with previous $Co^{III}(MPC)$ compounds, $[1]^{2^+}$ maintains the *trans-III* conformation of the macrocyclic ring with equatorial methyl and phenyl substituents. The Co centers exhibit pseudo-octahedral geometries with the four nitrogen members of the macrocyclic ring forming the equatorial plane and alkynyl/chloro ligands in the axial sites.

It was postulated in previous work that the long Co-N bonds and shorter Co axial bonds were the result of replacing cyclam with the MPC ligand.⁵³ As shown in Table 1, this structural feature remains true for $[1]^{2+}$, with the elongation of

Scheme 1. Synthetic Route to Prepare [1]Cl₂, [2]Cl₂, and [3]Cl₂^a

Table 1. Comparison of Bond Lengths and Angles for $[1]^{2+}$ and $[\{Co(cyclam)Cl\}_2(\mu-C_4)]^{2+}$ (cyclam)

$ \begin{array}{c ccccccccccccccccccccccccccccccccccc$			
$ \begin{array}{cccccccccccccccccccccccccccccccccccc$		[1] ²⁺	cyclam ^a
Co1-C1 1.874(2) 1.878(4) Co2-C4 1.875(2) 1.890(5) C1-C2 1.211(2) 1.208(6) C2-C3 1.376(2) 1.388(5) C3-C4 1.209(2) 1.201(5) Cl1-Co1-C1 178.92(5) 177.25(13) Cl2-Co2-C4 177.57(6) 177.49(12) Co1-C1-C2 177.48(2) 170.1(4) Co2-C4-C3 174.27(2) 169.3(4)	Co-N _{avg}	1.996[1]	1.977[3]
Co2-C4 1.875(2) 1.890(5) C1-C2 1.211(2) 1.208(6) C2-C3 1.376(2) 1.388(5) C3-C4 1.209(2) 1.201(5) Cl1-Co1-C1 178.92(5) 177.25(13) Cl2-Co2-C4 177.57(6) 177.49(12) Co1-C1-C2 177.48(2) 170.1(4) Co2-C4-C3 174.27(2) 169.3(4)	Co-Cl _{avg}	2.2978[5]	2.3137[11]
C1-C2 1.211(2) 1.208(6) C2-C3 1.376(2) 1.388(5) C3-C4 1.209(2) 1.201(5) Cl1-Co1-C1 178.92(5) 177.25(13) Cl2-Co2-C4 177.57(6) 177.49(12) Co1-C1-C2 177.48(2) 170.1(4) Co2-C4-C3 174.27(2) 169.3(4)	Co1-C1	1.874(2)	1.878(4)
C2-C3 1.376(2) 1.388(5) C3-C4 1.209(2) 1.201(5) Cl1-Co1-C1 178.92(5) 177.25(13) Cl2-Co2-C4 177.57(6) 177.49(12) Co1-C1-C2 177.48(2) 170.1(4) Co2-C4-C3 174.27(2) 169.3(4)	Co2-C4	1.875(2)	1.890(5)
C3-C4 1.209(2) 1.201(5) Cl1-Co1-C1 178.92(5) 177.25(13) Cl2-Co2-C4 177.57(6) 177.49(12) Co1-C1-C2 177.48(2) 170.1(4) Co2-C4-C3 174.27(2) 169.3(4)	C1-C2	1.211(2)	1.208(6)
CI1-Co1-C1 178.92(5) 177.25(13) CI2-Co2-C4 177.57(6) 177.49(12) Co1-C1-C2 177.48(2) 170.1(4) Co2-C4-C3 174.27(2) 169.3(4)	C2-C3	1.376(2)	1.388(5)
Cl2-Co2-C4 177.57(6) 177.49(12) Co1-C1-C2 177.48(2) 170.1(4) Co2-C4-C3 174.27(2) 169.3(4)	C3-C4	1.209(2)	1.201(5)
Co1-C1-C2 177.48(2) 170.1(4) Co2-C4-C3 174.27(2) 169.3(4)	Cl1-Co1-C1	178.92(5)	177.25(13)
Co2-C4-C3 174.27(2) 169.3(4)	Cl2-Co2-C4	177.57(6)	177.49(12)
	Co1-C1-C2	177.48(2)	170.1(4)
Taken from ref 49.	Co2-C4-C3	174.27(2)	169.3(4)
	Γaken from ref 49.		

Co–N bonds and shortening of Co axial bonds relative to those of $[\{Co(cyclam)Cl\}_2(\mu\text{-}C_4)]^{2^+}$. Consequently, the alkynyl C≡C bonds are lengthened, and the C–C single bond is shortened, indicating a small but discernible contribution of the cumulenic resonance structure.

Voltammetric Studies. The $Co^{III/II}$ couple of previously studied $[Co(MPC)(C_2Ph)_2]^+$ is quasi-reversible. Whereas that of $[Co(cyclam)(C_2Ph)_2]^+$ is irreversible. The concurrent weakening of MPC coordination and strengthening of axial bonds have a clear impact on the electronics of the dicobalt species, as shown by the cyclic voltammograms (CV) and differential pulse voltammograms (DPV) of complexes $[1]^{2+}-[3]^{2+}$ in Figure 2. In $Co^{III}(cyclam)$ -based complexes, the

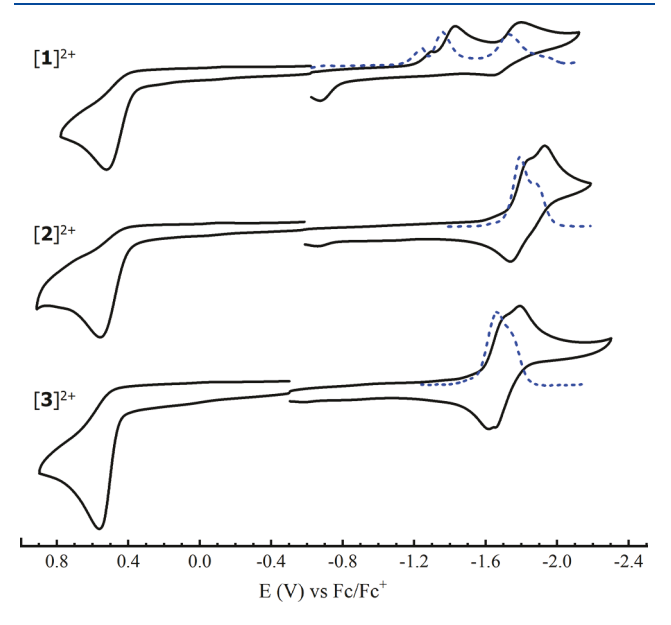


Figure 2. CVs (black, solid) and DPVs (blue, dashed) of 1.0 mM $[1]^{2+}$, $[2]^{2+}$, and $[3]^{2+}$ recorded in 0.1 M Bu₄NPF₆ MeCN solution at a scan rate of 0.10 V/s.

chloro ligand tends to dissociate upon reduction, resulting in irreversibility of the Co^{III/II} redox couple. The CV of [1]²⁺ shares this feature with two irreversible reductions at $-1.39~V~(Co^{III/II})$ and $-1.76~V~(Co^{II/I})$ and an irreversible oxidation at 0.52 V $(Co^{IV/III})~(Table~2)$. The CV and DPV of [2]²⁺ are substantially different from those of [{Co(cyclam)(C₂Ph)}₂(μ -C₄)]^{2+,51} The Co^{III/II} couples are the only observable reduction events within the cathodic end of the solvent window, and are

Table 2. Reduction Potentials (V vs $Fc^{+/0}$) for $[1]^{2+}$, $[2]^{2+}$, and $[3]^{2+}$

Е	$[1]^{2+}$	$[2]^{2+}$	$[3]^{2+}$
$E_{\rm pa} \ 4 + /2 +$	0.52	0.56	0.64
$E_{\rm pc} 2 + /1 +$	-1.39^{a}	-1.79^{b}	-1.65^{b}
$E_{\rm pc} \ 1 + /0$		-1.89^{b}	-1.74^{b}
$E_{\rm pc} \ 0/2-$	-1.76		
$E(2+/1+) (BArF_{24})^{c}$		-1.75	-1.66
$E(1+/0) (BArF_{24})^c$		-1.91	-1.81

^aPotential for a 2-electron 2+/0 process. ^bDetermined from deconvoluted DPV. ^cDetermined using NBu₄BArF electrolyte

both quasi-reversible and clearly two separated one electron processes. The second reduction has a lower peak current than the first, indicating a partial chemical degradation after the first reduction. The oxidation ($\text{Co}^{\text{IV/III}}$) appears as a two-electron process at 0.56 V.

Compound [3]Cl₂ was prepared with the goal of increasing the stability of the reduced state by combining the effects seen from electron-withdrawing ligands with the effect of the MPC ligand. In this regard, $[3]^{2+}$ is more electrochemically stable than [2]2+, with a larger return wave and absence of the degradation peak around -0.55 V seen in the other two compounds (Figure 2). The reduction peaks were found to be separated by 0.09 V, located at -1.65 and -1.74 V, with the second reduction being 90% the size of the first reduction (Figure S4). The increased electron-withdrawing effect of the 3,5-dichloro substituents shifts the reduction of $[3]^{2+}$ to a more anodic value than that of $[2]^{2+}$, indicating the increased electron deficiency at the Co centers. While the enhanced coordination of the 3,5-dichlorophenylacetylide ligand improves stability of the reduced state, it also decreases the peak separation of each reduction when compared to $[2]^{2+}$ (0.10 V for $[2]^{2+}$, 0.09 V for $[3]^{2+}$), as was hypothesized in previous works. 49

The use of anions with low affinities for ion pairing as the electrolyte has been proven to improve separation of singleelectron reductions in mixed valence compounds by thermodynamically stabilizing the singly reduced state. 54,55 In order to improve the separation of the stepwise reduction processes in $[2]^{2+}$ and $[3]^{2+}$, NBu_4BArF (NBu_4BArF = tetrabutylammonium tetrakis[3,5-bis(trifluoromethyl)phenyl]borate) was employed as the electrolyte in place of NBu₄PF₆, using dichloromethane as a noncoordinating solvent. As shown in Figure 3, the electrochemical stability of the singly reduced states of both $[2]^{2+}$ and $[3]^{2+}$ in the cathodic window improved significantly. For $[2]^{2+}$, the first and second redox waves are well-defined at -1.69 and -1.85 V, respectively, and the stability is much improved, judging from the equal currents of each reduction in the DPV. For [3]²⁺, the reduction couples are more reversible than those of [2]2+ with the first and second couples at -1.62 and -1.77 V, respectively. Finally, the well-resolved DPV waves allow for an unambiguous determination of the separation between the two stepwise one-electron reductions as 160 mV for [2]²⁺ and 150 mV [3]²⁺.

Density Functional Theory (DFT) Calculations. To gain further insight into the electronic structures, DFT calculations/ analysis were performed for complexes $[1]^{2+}$, $[2]^{2+}$, and $[3]^{2+}$. In the absence of suitable crystal structures for $[2]^{2+}$ and $[3]^{2+}$, all DFT calculations were based on the molecular structure of $[1]^{2+}$ with appropriate modifications whenever necessary. The frontier orbitals and energy levels for $[1]^{2+}$ and $[2]^{2+}$ are

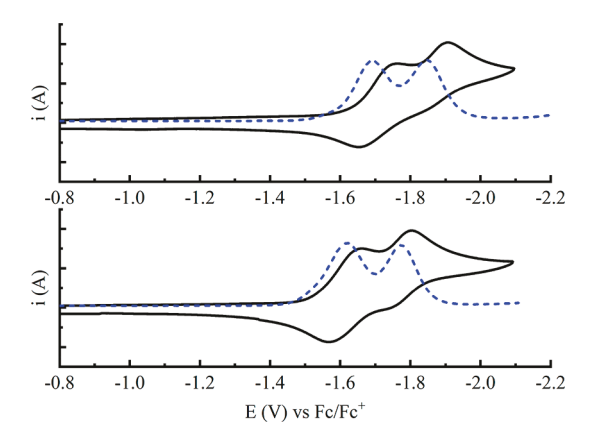


Figure 3. CVs (black, solid) and DPVs (blue, dashed) for 1 mM $[2]^{2+}$ (top) or $[3]^{2+}$ (bottom) recorded in 0.1 M Bu₄BArF CH₂Cl₂ solutions.

displayed in Figure 4. Those of [3]²⁺ are given in Figure S5, and relevant bonds lengths are given in Table S2.

Complexes $[1]^{2+}$, $[2]^{2+}$, and $[3]^{2+}$ share the same feature in their LUMO-LUMO+3, with the LUMO and LUMO+1 consisting of the $d_{x^2-y^2}$ orbitals and LUMO+2 and LUMO+3 consisting of the d_{z^2} orbitals. This feature is consistent with the e_g set of orbitals for a low-spin, pseudo-octahedral, d⁶ Co^{III} center. The stabilization of $d_{x^2-y^2}$ orbitals over the d_{z^2} orbitals is clearly a manifestation of weaker ligand field in the xy plane exerted by the MPC ligand. In contrast, the dz2 orbitals dominate the LUMO and LUMO+1 of [{Co(cyclam)Cl}₂(μ - $(C_4)^{2+}$, which are σ^* (Co axial ligand) in nature. ⁴⁹ Hence, while the reduction of $[\{Co(cyclam)Cl\}_2(\mu-C_4)]^{2+}$ is followed by the dissociation of one of the axial ligands (likely Cl⁻), the reduction of $[\{Co(MPC)(C_2Ar)\}_2(\mu-C_4)]^{2+}$ populates the $d_{x^2-y^2}$ orbitals, which does not lead to the dissociation of arylacetylide and thus enhances electrochemical reversibility. However, the highest occupied orbitals in the MPC-based complexes are similar to those of $[{Co(cyclam)Cl}_2(\mu$ - $(C_4)^{2+49}$ For $[1]^{2+}$, the HOMO and HOMO-1 are the

mixtures of the d_{xz} and d_{yz} orbitals with the $\pi(C \equiv C)$ orbitals of the butadiyndiyl bridge. For $[2]^{2+}$ and $[3]^{2+}$, the mixtures of the d_{xz} and d_{yz} orbitals with the $\pi(C \equiv C)$ orbitals of capping arylacetylide ligands dominate the HOMO and HOMO-1, while the mixtures of the d_{xz} and d_{yz} orbitals with the $\pi(\text{bridge})$ orbitals result in the orbitals HOMO-2 and HOMO-3. Although LUMO/LUMO+1 in $[2]^{2+}$ and $[3]^{2+}$ are the localized $d_{x^2-y^2}$ orbitals with no obvious Co-Co interaction, two Co^{III} centers can still engage in significant electronic coupling manifested by the HOMO-2 and HOMO-3 via a hole-transfer formalism outlined by Launay.^{7,8}

CONCLUSION

A series of Co^{III}(MPC) alkynyl complexes have been prepared in modest to high yields. The alkynyl-capped compounds [2]²⁺ and [3]²⁺ are the first examples of cyclam-based complexes which display unambiguous intermetallic coupling across an oligoyne bridge. Furthermore, [2]²⁺ is the first such cobalt cyclam-derived complex to have a quasi-stable reduced state without the use of electron-withdrawing axial ligands. These properties are the result of weaker coordination of the MPC ligand when compared to those of cyclam, which allows for enhanced axial ligand binding. The combined effects of electron-withdrawing arylacetylides and the weakened equatorial ligand field by the MPC ligand resulted in two reversible one electron reductions in [3]2+, a rarity in CoIII redox chemistry. Compounds bearing more electron-deficient macrocyclic ligands that retain the steric bulk of MPC are being developed in our laboratory to fully elaborate the effect of LUMO engineering through the tuning of equatorial ligand field strength.

EXPERIMENTAL SECTION

Materials. The synthesis for [Co(MPC)Cl₂]Cl was described previously.⁵³ 3,5-Dichlorophenylacetylene was prepared according to a literature procedure.⁵⁶ Bis(trimethylsilyl)butadiyne was purchased from GFS Chemicals. *n*-BuLi was purchased from Aldrich. Lithium diisopropylamide was prepared in situ by addition of *n*-BuLi to

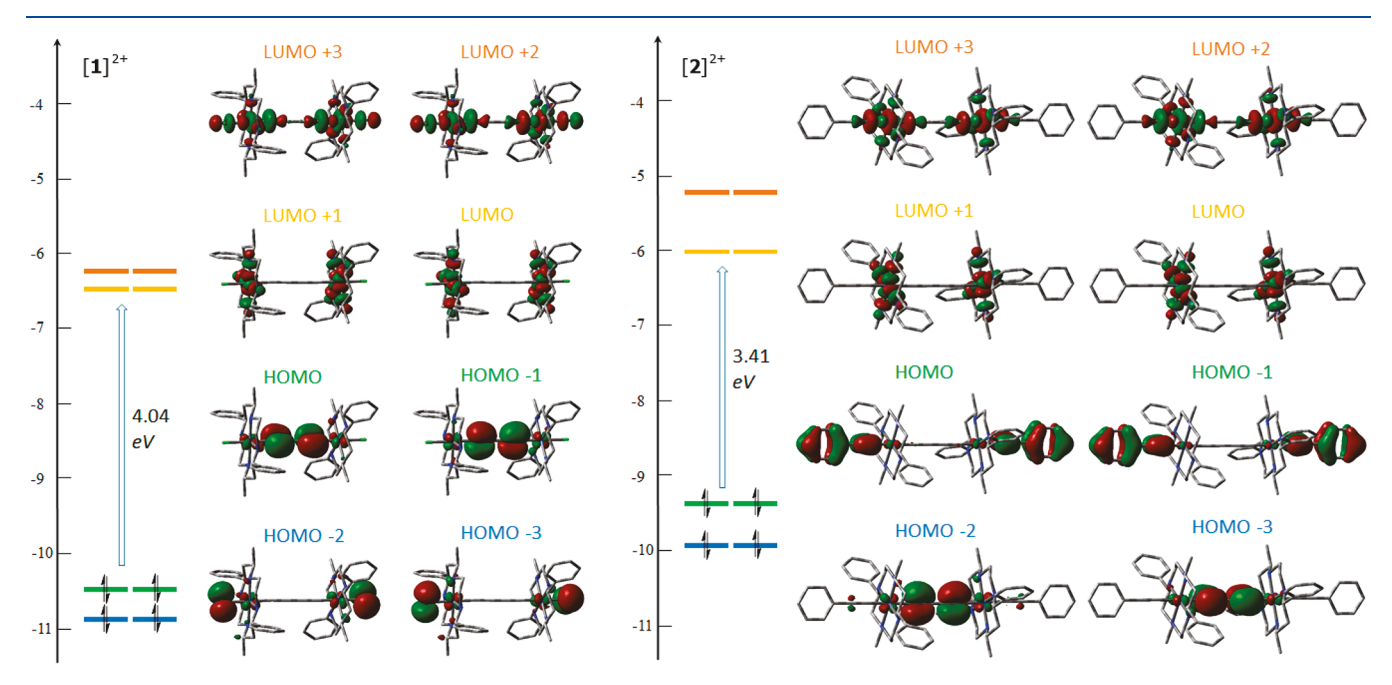


Figure 4. Molecular orbital diagrams for [1]²⁺ and [2]²⁺ from DFT calculations. The isovalue of the contour plots was set at 0.03.

distilled diisopropylamine. All reagents were used as received. Tetrahydrofuran was freshly distilled over sodium/benzophenone. All lithiation reactions were carried out under N_2 using standard Schlenk techniques.

Physical Measurements. $^1\mathrm{H}$ NMR spectra were obtained with a Varian Mercury300 NMR instrument, with chemical shifts (δ) referenced to the residual solvent signal (CHCl $_3$ at $\delta=7.26$ ppm). UV/vis spectra were obtained with a JASCO V-670 spectrophotometer. FT-IR spectra were measured as neat samples using a JASCO FT/IR-6300 spectrometer equipped with an ATR accessory. Electrospray mass spectra were obtained as electrospray in positive-ion mode with the aid of an Advion Expression Compact Mass Spectrometer. Elemental analysis was carried out by Atlantic Micro Laboratories in Norcross, GA. Electrochemical analysis was done on a CHI620A voltammetric analyzer with a glassy carbon working electrode (diameter = 2 mm), a Pt-wire auxiliary electrode, and a Ag/AgCl reference electrode. The analyte concentration is 1.0 mM in 4 mL of dry acetonitrile with a 0.1 M Bu $_4\mathrm{NPF}_6$ electrolyte concentration, unless otherwise stated.

Synthesis of $[\{Co(MPC)Cl\}_2(\mu-C_4)]Cl_2$ ([1]Cl₂). To a methanolic solution of [Co(MPC)Cl₂]Cl (1.00 g, 1.83 mmol) was added triethylamine (5.0 mL, 36 mmol), followed by a THF solution of bis(trimethylsilyl)butadiyne (0.188 g, 0.967 mmol). The solution was allowed to reflux for 24 h as the color turned from green to orange to red. The solvent was removed via rotary evaporation, and the residue was purified on silica gel with a gradient of CH2Cl2-MeOH, gradually proceeding from pure CH₂Cl₂ to a 9:1 ratio of CH₂Cl₂ to MeOH. The collected red product was recrystallized from CH₂Cl₂-Et₂O. Yield: 0.435 g, (44% based on Co). ESI-MS (MeCN): 498 $[\{Co(MPC)Cl\}_2(\mu-C_4)]^{2+}$. Elem. Anal. for $C_{54}H_{80}N_8O_2Co_2Cl_8$ ([1]Cl₂·2H₂O·2CH₂Cl₂): calcd C 50.88, H 6.32, N 8.79. Found C 50.54, H 6.64, N 8.91. 1 H NMR (CDCl₃, δ): 8.29 (br, 2 H, NH), 7.60-7.10 (m, 20 H, ArH), 6.12 (br, 2 H, NH), 5.57 (br, 2 H, NH), 4.44 (m, 2 H, CH), 4.23 (m, 4 H, CH₂), 3.74 (m, 2 H), 3.58 (br, 2 H, NH), 3.37 (m, 2 H), 3.11 (m, 6 H), 2.79 (m, 4 H), 2.27 (m, 6 H), 1.99 (dd, 2 H), 1.83 (m, 4 H), 1.48 (d, 6 H, CH₃), 1.35 (d, 6 H, CH₃) ppm. UV-vis spectra, λ_{max} (nm, ε (M⁻¹ cm⁻¹)): 207 (66 000), 233 (74 000), 350 (3100), 520 (380).

Synthesis of $[\{Co(MPC)(C_2Ph)\}_2(\mu-C_4)]Cl_2$ ([2]Cl₂). A solution of [1]Cl₂ (83 mg, 0.078 mmol) in THF was combined with a solution of Li-phenylacetylide (prepared from 0.36 mmol phenylacetylene and 0.50 mmol LDA) in THF at -78 °C. This was allowed to warm to room temperature and stirred 12 h before quenching with air and removal of solvent via rotary evaporation. The residue was purified on silica gel with a 15:1 ratio of CH2Cl2:MeOH. The collected orange fraction was recrystallized from CH2Cl2-Et2O, yielding 63 mg (68% based on Co). ESI-MS (MeCN): 564 $[\{Co(MPC)(C_2Ph\}_2(\mu-C_4)]^{2+}$. Elem. Anal. for C_{71.5}H₈₉N₈Co₂Cl₉ ([2]Cl₂·3.5CH₂Cl₂): calcd C 57.35, H 5.99, N 7.48. Found C 57.17, H 5.99, N 7.48. ¹H NMR (CDCl₃, δ): 8.29 (br, 2 H, NH), 7.65–7.05 (m, 30 H, ArH), 5.49 (br, 2 H, NH), 4.91 (br, 2 H, NH), 4.22 (m, 4 H), 4.00 (t, 2 H), 3.62 (br, 2 H, NH), 3.41 (m, 4 H), 3.02 (m, 6 H), 2.86 (m, 2 H), 2.65-2.05 (m, 8 H), 1.94 (dd, 2 H), 1.72 (m, 4 H), 1.42 (d, 6 H, CH₃), 1.37 (d, 6 H, CH₃) ppm. UV-vis spectra, λ_{max} (nm, ε (M⁻¹ cm⁻¹)): 224 (92 000), 260 (74 000), 349 (2,700), 484 (340).

Synthesis of [{Co(MPC)(3,5-ClC₂Ph)}₂(μ -C₄)]Cl₂ ([3]Cl₂). A solution of [1]Cl₂ (86 mg, 0.080 mmol) in THF was combined with a solution of Li-3,5-dichlorophenylacetylide (prepared from 0.36 mmol of 3,5-dichlorophenylacetylene and 0.50 mmol of LDA) in THF at -78 °C. This was allowed to warm to room temperature and stirred for 12 h before quenching with air and removal of solvent via rotary evaporation. The residue was purified on silica gel with a 24:1 ratio of CH₂Cl₂-MeOH. The collected orange fraction was recrystallized from CH₂Cl₂/Et₂O, yielding 56 mg (52% based on Co). ESI-MS (MeCN): 633 [{Co(MPC)(3,5-ClC₂Ph)}₂(μ -C₄)]²⁺. Elem. Anal. for C₆₉H₈₂N₈O₁Co₂Cl₈ ([3]Cl₂·H₂O·CH₂Cl₂): calcd C 57.52, H 5.74, N 7.77. Found C 57.34, H 5.89, N 7.51. ¹H NMR (CDCl₃, δ): 7.99 (br, 2 H, NH), 7.80–7.00 (m, 26 H, ArH), 5.57 (br, 2 H, NH), 4.84 (br, 2 H, NH), 4.22 (t, 2 H), 4.09 (m, 2 H), 3.85 (t, 2 H), 3.70–3.20 (m, 6 H), 3.15–2.85 (m, 6 H), 2.68–2.28 (m, 6 H),

2.17 (m, 4 H), 1.94 (dd, 2 H), 1.74 (m, 4 H), 1.40 (m, 12 H, CH₃) ppm. UV–vis spectra, $\lambda_{\rm max}$ (nm, ε (M⁻¹ cm⁻¹)): 226 (100 000), 279 (62 000), 349 (2500), 479 (320).

Computational Details. The geometries of $[1]^{2+}$, $[2]^{2+}$, and $[3]^{2+}$ in the ground states were fully optimized based on the crystal structure of $[1](BPh_4)_2$. Both $[2]^{2+}$ and $[3]^{2+}$ had the additional ligands manually edited without changing the rest of the structure. The density functional method B3LYP (Beck's three-parameter hybrid functional using the Lee—Yang—Parr correlation functional)⁵⁷ was used for calculations with the def2-TZVP basis set used for cobalt, and the def2-SVP basis set was used for all other atoms.⁵⁸ The calculation was accomplished by using the Gaussian16 program package.⁵⁹

X-ray Crystallographic Analysis. Single-crystal X-ray data was collected on a Bruker AXS D8 Quest CMOS diffractometer using Mo $K\alpha$ ($\lambda=0.71073$ Å) radiation with Apex3 software. Data was reduced using SAINT and structures were solved with SHELXTL. Refinement was performed with SHELXL. ORTEP plots were produced using SHELXTL.

ASSOCIATED CONTENT

Supporting Information

The Supporting Information is available free of charge at https://pubs.acs.org/doi/10.1021/acs.organomet.0c00183.

Experimental crystallographic details, and supramolecular structure plots for 1; DPV plot for $[1]^{2+}$; DPV peak deconvolution for $[2]^{2+}$ and $[3]^{2+}$; orbital splitting diagram from DFT calculations for $[3]^{2+}$; bond lengths and angles from DFT calculations for all presented complexes; NMR, UV—vis, and IR for all complexes (PDF)

Accession Codes

CCDC 1991075 contains the supplementary crystallographic data for this paper. These data can be obtained free of charge via www.ccdc.cam.ac.uk/data_request/cif, or by emailing data_request@ccdc.cam.ac.uk, or by contacting The Cambridge Crystallographic Data Centre, 12 Union Road, Cambridge CB2 1EZ, UK; fax: +44 1223 336033.

AUTHOR INFORMATION

Corresponding Author

Tong Ren — Department of Chemistry, Purdue University, West Lafayette, Indiana 47907, United States; orcid.org/0000-0002-1148-0746; Email: tren@purdue.edu

Authors

Brandon L. Mash — Department of Chemistry, Purdue University, West Lafayette, Indiana 47907, United States Yiwei Yang — Department of Chemistry, Purdue University, West Lafayette, Indiana 47907, United States

Complete contact information is available at: https://pubs.acs.org/10.1021/acs.organomet.0c00183

Notes

The authors declare no competing financial interest.

ACKNOWLEDGMENTS

We thank the National Science Foundation for generously supporting this work (CHE 1764347 for research and CHE 1625543 for X-ray diffractometers), and Mr. R. A. Clendening and Mr. A. Raghavan for experimental assistance.

REFERENCES

- (1) Nast, R. Zur Existenz Metallorganischer Verbindungen Von Ubergangsmetallen. Z. Naturforsch., B: J. Chem. Sci. 1953, 8, 381.
- (2) Nast, R. Coordination Chemistry of Metal Alkynyl Compounds. Coord. Chem. Rev. 1982, 47, 89–124.
- (3) Haque, A.; Al-Balushi, R. A.; Al-Busaidi, I. J.; Khan, M. S.; Raithby, P. R. Rise of Conjugated Poly-ynes and Poly(Metalla-ynes): From Design Through Synthesis to Structure—Property Relationships and Applications. *Chem. Rev.* **2018**, *118*, 8474—8597.
- (4) Wong, W.-Y.; Ho, C.-L. Organometallic Photovoltaics: A New and Versatile Approach for Harvesting Solar Energy Using Conjugated Polymetallaynes. *Acc. Chem. Res.* **2010**, *43*, 1246–1256.
- (5) Ho, C.-L.; Yu, Z.-Q.; Wong, W.-Y. Multifunctional polymetallaynes: properties, functions and applications. *Chem. Soc. Rev.* **2016**, 45, 5264–5295.
- (6) Haque, A.; Xu, L. L.; Al-Balushi, R. A.; Al-Suti, M. K.; Ilmi, R.; Guo, Z. L.; Khan, M. S.; Wong, W. Y.; Raithby, P. R. Cyclometallated tridentate platinum(II) arylacetylide complexes: old wine in new bottles. *Chem. Soc. Rev.* **2019**, *48*, 5547–5563.
- (7) Launay, J.-P. Long-distance intervalence electron transfer. *Chem. Soc. Rev.* **2001**, *30*, 386–397.
- (8) Launay, J. P. Mixed-Valent Compounds and their Properties Recent Developments. Eur. J. Inorg. Chem. 2020, 2020, 329–341.
- (9) Szafert, S.; Gladysz, J. A. Carbon in One Dimension: Structural Analysis of the Higher Conjugated Polyynes. *Chem. Rev.* **2003**, *103*, 4175–4206.
- (10) Szafert, S.; Gladysz, J. A. Update 1 of: Carbon in One Dimension: Structural Analysis of the Higher Conjugated Polyynes. *Chem. Rev.* **2006**, *106*, PR1–PR33.
- (11) Halet, J. F.; Lapinte, C. Charge delocalization vs localization in carbon-rich iron mixed-valence complexes: A subtle interplay between the carbon spacer and the (dppe)Cp*Fe organometallic electrophore. *Coord. Chem. Rev.* **2013**, 257, 1584–1613.
- (12) Gendron, F.; Groizard, T.; Le Guennic, B.; Halet, J. F. Electronic Properties of Poly-Yne Carbon Chains and Derivatives with Transition Metal End-Groups. *Eur. J. Inorg. Chem.* **2020**, 2020, 667–681.
- (13) Costuas, K.; Rigaut, S. Polynuclear carbon-rich organometallic complexes: clarification of the role of the bridging ligand in the redox properties. *Dalton Trans.* **2011**, *40*, 5643–5658.
- (14) Tanaka, Y.; Akita, M. Organometallic radicals of iron and ruthenium: Similarities and dissimilarities of radical reactivity and charge delocalization. *Coord. Chem. Rev.* **2019**, 388, 334–342.
- (15) Le Narvor, N.; Lapinte, C. First C₄ Bridged Mixed-valence Iron(II)-Iron(III) Complex Delocalized on the Infrared Timescale. *J. Chem. Soc., Chem. Commun.* **1993**, *0*, 357–359.
- (16) Fernández, F. J.; Venkatesan, K.; Blacque, O.; Alfonso, M.; Schmalle, H. W.; Berke, H. Generation and Coupling of [Mn(dmpe)-2(CCR)(CC)]. Radicals Producing Redox-Active C4-Bridged Rigid-Rod Complexes. *Chem. Eur. J.* **2003**, *9*, 6192–6206.
- (17) Bruce, M. I.; Low, P. J.; Costuas, K.; Halet, J.-F.; Best, S. P.; Heath, G. A. Oxidation Chemistry of Metal-Bonded C4 Chains: A Combined Chemical, Spectroelectrochemical, and Computational Study. *J. Am. Chem. Soc.* **2000**, *122*, 1949–1962.
- (18) Ren, T.; Zou, G.; Alvarez, J. C. Facile Electronic Communication between Bimetallic Termini Bridged by Elemental Carbon Chains. *Chem. Commun.* **2000**, 1197–1198.
- (19) Wong, K.-T.; Lehn, J.-M.; Peng, S.-M.; Lee, G.-H. Nanoscale molecular organometallo-wires containing diruthenium cores. *Chem. Commun.* **2000**, 2259–2260.
- (20) Ren, T. Diruthenium σ -Alkynyl Compounds: A New Class of Conjugated Organometallics. *Organometallics* **2005**, 24, 4854–4870.
- (21) Zhou, Y. L.; Seyler, J. W.; Weng, W.; Arif, A. M.; Gladysz, J. A. New Families of Coordinated Carbon: Oxidative Coupling of an Ethynyl Complex to Isolable and Crystallographically Characterized MC = CC = CM amd + MC = CC = CM+ Assemblies. *J. Am. Chem. Soc.* 1993, 115, 8509–8510.
- (22) Dembinski, R.; Bartik, T.; Bartik, B.; Jaeger, M.; Gladysz, J. A. Toward Metal-Capped One-Dimensional Carbon Allotropes: Wire-

- like C6-C20 Polyynediyl Chains That Span Two Redox-Active ([Image]5-C5Me5)Re(NO)(PPh3) Endgroups. *J. Am. Chem. Soc.* **2000**, *122*, 810–822.
- (23) Schull, T. L.; Kushmerick, J. G.; Patterson, C. H.; George, C.; Moore, M. H.; Pollack, S. K.; Shashidhar, R. Ligand Effects on Charge Transport in Platinum(II) Acetylides. *J. Am. Chem. Soc.* **2003**, *125*, 3202–3203.
- (24) Ballmann, S.; Hieringer, W.; Secker, D.; Zheng, Q.; Gladysz, J. A.; Görling, A.; Weber, H. B. Molecular Wires in Single-Molecule Junctions: Charge Transport and Vibrational Excitations. *ChemPhysChem* **2010**, *11*, 2256–2260.
- (25) Tanaka, Y.; Kato, Y.; Tada, T.; Fujii, S.; Kiguchi, M.; Akita, M. "Doping" of Polyyne with an Organometallic Fragment Leads to Highly Conductive Metallapolyyne Molecular Wire. *J. Am. Chem. Soc.* **2018**, *140*, 10080–10084.
- (26) Kim, B.; Beebe, J. M.; Olivier, C.; Rigaut, S.; Touchard, D.; Kushmerick, J. G.; Zhu, X.-Y.; Frisbie, C. D. Temperature and Length Dependence of Charge Transport in Redox-Active Molecular Wires Incorporating Ruthenium(II) Bis(-arylacetylide) Complexes. *J. Phys. Chem. C* 2007, 111, 7521–7526.
- (27) Ezquerra, R.; Eaves, S. G.; Bock, S.; Skelton, B. W.; Perez-Murano, F.; Cea, P.; Martin, S.; Low, P. J. New routes to organometallic molecular junctions via a simple thermal processing protocol. *J. Mater. Chem. C* **2019**, *7*, 6630–6640.
- (28) Blum, A. S.; Ren, T.; Parish, D. A.; Trammell, S. A.; Moore, M. H.; Kushmerick, J. G.; Xu, G.-L.; Deschamps, J. R.; Pollack, S. K.; Shashidhar, R. $R_2(ap)_4(\sigma-oligo(phenyleneethynyl))$ Molecular Wires: Synthesis and Electronic Characterization. *J. Am. Chem. Soc.* **2005**, *127*, 10010–10011.
- (29) Mahapatro, A. K.; Ying, J.; Ren, T.; Janes, D. B. Electronic Transport through Ruthenium Based Redox-Active Molecules in Metal-Molecule-Metal Nanogap Junctions. *Nano Lett.* **2008**, *8*, 2131–2136.
- (30) Zhu, H.; Pookpanratana, S. J.; Bonevich, J. E.; Natoli, S. N.; Hacker, C. A.; Ren, T.; Suehle, J. S.; Richter, C. A.; Li, Q. Redox-Active Molecular Nanowire Flash Memory for High-Endurance and High-Density Non-Volatile Memory Applications. *ACS Appl. Mater. Interfaces* **2015**, *7*, 27306–27313.
- (31) Jiang, K.; Pookpanratana, S. J.; Natoli, S. N.; Ren, T.; Sperling, B. A.; Robertson, J.; Richter, C. A.; Yu, S.; Li, Q. Nonvolatile memory based on redox-active Ruthenium molecular monolayers. *Appl. Phys. Lett.* **2019**, *115*, No. 162102.
- (32) Meng, F. B.; Hervault, Y. M.; Norel, L.; Costuas, K.; Van Dyck, C.; Geskin, V.; Cornil, J.; Hng, H. H.; Rigaut, S.; Chen, X. D. Photomodulable molecular transport junctions based on organometallic molecular wires. *Chem. Sci.* **2012**, *3*, 3113–3118.
- (33) Meng, F. B.; Hervault, Y. M.; Shao, Q.; Hu, B. H.; Norel, L.; Rigaut, S.; Chen, X. D. Orthogonally modulated molecular transport junctions for resettable electronic logic gates. *Nat. Commun.* **2014**, *5*, No. 3023.
- (34) Ren, T. Sustainable metal alkynyl chemistry: 3d metals and polyaza macrocyclic ligands. *Chem. Commun.* **2016**, 52, 3271–3279.
- (35) Banziger, S. D.; Ren, T. Syntheses, Structures and Bonding of 3d Metal Alkynyl Complexes of Cyclam and Its Derivatives. *J. Organomet. Chem.* **2019**, 885, 39–48.
- (36) Hoffert, W. A.; Kabir, M. K.; Hill, E. A.; Mueller, S. M.; Shores, M. P. Stepwise acetylide ligand substitution for the assembly of ethynylbenzene-linked Co(III) complexes. *Inorg. Chim. Acta* **2012**, 380, 174–180.
- (37) Hoffert, W. A.; Shores, M. P. Crystallographic coincidence of two bridging species in a dinuclear CoIII ethynylbenzene complex. *Acta Crystallogr., Sect. E: Struct. Rep. Online* **2011**, *67*, m853–m854.
- (38) Nishijo, J.; Judai, K.; Numao, S.; Nishi, N. Chromium Acetylide Complex Based Ferrimagnet and Weak Ferromagnet. *Inorg. Chem.* **2009**, *48*, 9402–9408.
- (39) Nishijo, J. Chromium-ethynyltetrathiafulvalene complex based magnetic materials. *Polyhedron* **2013**, *66*, 43–47.
- (40) Nishijo, J.; Judai, K.; Nishi, N. Weak Ferromagnetism and Strong Spin-Spin Interaction Mediated by the Mixed-Valence

- Ethynyltetrathiafulvalene-Type Ligand. *Inorg. Chem.* **2011**, *50*, 3464–3470.
- (41) Nishijo, J.; Enomoto, M. A Series of Weak Ferromagnets Based on a Chromium-Acetylide-TTF Type Complex: Correlation of the Structures and Magnetic Properties and Origin of the Weak Ferromagnetism. *Inorg. Chem.* **2013**, *52*, 13263–13268.
- (42) Nishijo, J.; Enomoto, M. Synthesis, structure and magnetic properties of [CrCyclam(C C-6-methoxynaphthalene) 2](TCNQ) n (1,2-dichloroethane) (n = 1, 2). *Inorg. Chim. Acta* **2015**, *437*, 59–63.
- (43) Eddy, L. E.; Thakker, P. U.; McMillen, C. D.; Pienkos, J. A.; Cordoba, J. J.; Edmunds, C. E.; Wagenknecht, P. S. A comparison of the metal-ligand interactions of the pentafluorophenylethynyl and trifluoropropynyl ligands in transition metal cyclam complexes. *Inorg. Chim. Acta* 2019, 486, 141–149.
- (44) Grisenti, D. L.; Thomas, W. W.; Turlington, C. R.; Newsom, M. D.; Priedemann, C. J.; VanDerveer, D. G.; Wagenknecht, P. S. Emissive Chromium(III) Complexes with Substituted Arylethynyl Ligands. *Inorg. Chem.* **2008**, *47*, 11452–11454.
- (45) Sun, C.; Turlington, C. R.; Thomas, W. W.; Wade, J. H.; Stout, W. M.; Grisenti, D. L.; Forrest, W. P.; VanDerveer, D. G.; Wagenknecht, P. S. Synthesis of cis and trans Bis-alkynyl Complexes of Cr(III) and Rh(III) Supported by a Tetradentate Macrocyclic Amine: A Spectroscopic Investigation of the M(III)–Alkynyl Interaction. *Inorg. Chem.* 2011, 50, 9354−9364.
- (46) Sun, C.; Thakker, P. U.; Khulordava, L.; Tobben, D. J.; Greenstein, S. M.; Grisenti, D. L.; Kantor, A. G.; Wagenknecht, P. S. Trifluoropropynyl as a Surrogate for the Cyano Ligand and Intense, Room-Temperature, Metal-Centered Emission from Its Rh(III) Complex. *Inorg. Chem.* **2012**, *51*, 10477–10479.
- (47) Thakker, P. U.; Sun, C.; Khulordava, L.; McMillen, C. D.; Wagenknecht, P. S. Synthetic control of the cis/trans geometry of [M(cyclam)(CCR)2]OTf complexes and photophysics of cis-[Cr-(cyclam)(CCCF3)2]OTf and cis-[Rh(cyclam)(CCCF3)2]OTf. J. Organomet. Chem. 2014, 772–773, 107–112.
- (48) Thakker, P. U.; Aru, R. G.; Sun, C.; Pennington, W. T.; Siegfried, A. M.; Marder, E. C.; Wagenknecht, P. S. Synthesis of trans bis-alkynyl complexes of Co(III) supported by a tetradentate macrocyclic amine: A spectroscopic, structural, and electrochemical analysis of π-interactions and electronic communication in the CCMCC structural unit. *Inorg. Chim. Acta* 2014, 411, 158−164.
- (49) Cook, T. D.; Natoli, S. N.; Fanwick, P. E.; Ren, T. CoIII(cyclam) Oligoynyls: Monomeric Oligoynyl Complexes and Dimeric Complexes with an Oligoyn-diyl Bridge. *Organometallics* **2016**, 35, 1329–1338.
- (50) Cook, T. D.; Natoli, S. N.; Fanwick, P. E.; Ren, T. Dimeric Complexes of CoIII(cyclam) with a Polyynediyl Bridge. *Organometallics* **2015**, *34*, 686–689.
- (51) Cook, T. D.; Fanwick, P. E.; Ren, T. Unsymmetric Mononuclear and Bridged Dinuclear CoIII(cyclam) Acetylides. *Organometallics* **2014**, 33, 4621–4624.
- (\$2) Natoli, S. N.; Zeller, M.; Ren, T. An Aerobic Synthetic Approach toward Bis-Alkynyl Cobalt(III) Compounds. *Inorg. Chem.* **2017**, *56*, 10021–10031.
- (53) Mash, B. L.; Ren, T. Co(III) phenylacetylide complexes supported by tetraazamacrocyclic ligands: Syntheses and characterizations. *J. Organomet. Chem.* **2019**, 880, 143–149.
- (54) Barriere, F.; Geiger, W. E. Use of weakly coordinating anions to develop an integrated approach to the tuning of Delta E-1/2 values by medium effects. *J. Am. Chem. Soc.* **2006**, *128*, 3980–3989.
- (55) Geiger, W. E.; Barriere, F. Organometallic Electrochemistry Based on Electrolytes Containing Weakly-Coordinating Fluoroarylborate Anions. *Acc. Chem. Res.* **2010**, *43*, 1030–1039.
- (56) Musso, D. L.; Clarke, M. J.; Kelley, J. L.; Evan Boswell, G.; Chen, G. Novel 3-phenylprop-2-ynylamines as inhibitors of mammalian squalene epoxidase. *Org. Biomol. Chem.* **2003**, *1*, 498–506
- (57) Parr, R. G.; Yang, W. B. Density Functional Theory of Atoms and Molecules; Oxford University Press: New York, 1989.

- (58) Weigend, F.; Ahlrichs, R. Balanced basis sets of split valence, triple zeta valence and quadruple zeta valence quality for H to Rn: Design and assessment of accuracy. *Phys. Chem. Chem. Phys.* **2005**, *7*, 3297–3305
- (59) Frisch, M. J.; Trucks, G. W.; Schlegel, H. B.; Scuseria, G. E.; Robb, M. A.; Cheeseman, J. R.; Scalmani, G.; Barone, V.; Petersson, G. A.; Nakatsuji, H.; Li, X.; Caricato, M.; Marenich, A. V.; Bloino, J.; Janesko, B. G.; Gomperts, R.; Mennucci, B.; Hratchian, H. P.; Ortiz, J. V.; Izmaylov, A. F.; Sonnenberg, J. L.; Williams-Young, D.; Ding, F.; Lipparini, F.; Egidi, F.; Goings, J.; Peng, B.; Petrone, A.; Henderson, T.; Ranasinghe, D.; Zakrzewski, V. G.; Gao, I.; Rega, N.; Zheng, G.; Liang, W.; Hada, M.; Ehara, M.; Toyota, K.; Fukuda, R.; Hasegawa, J.; Ishida, M.; Nakajima, T.; Honda, Y.; Kitao, O.; Nakai, H.; Vreven, T.; Throssell, K.; Montgomery, J. A., Jr.; Peralta, J. E.; Ogliaro, F.; Bearpark, M.; Heyd, J. J.; Brothers, E. N.; Kudin, K. N.; Staroverov, V. N.; Kobayashi, R.; Normand, J.; Raghavachari, K.; Rendell, A.; Burant, J. C.; Iyengar, S. S.; Tomasi, J.; Cossi, M.; Millam, J. M.; Klene, M.; Adamo, C.; Cammi, R.; Ochterski, J. W.; Martin, R. L.; Morokuma, K.; Farkas, O.; Foresman, J. B.; Fox, D. J. Gaussian 16, revision C.01; Gaussian, Inc.: Wallingford CT, 2016.
- (60) (a) Apex3 v2016.9-0; Bruker AXS Inc.: Madison, WI, 2016. (b) Saint V8.34A, V8.37A; Bruker AXS Inc.: Madison, WI, 2016.
- (61) SHELXTL, version 6.14; Bruker AXS Inc.: Madison, WI, 2000-2003.
- (62) Sheldrick, G. M. SHELXL 2016; University of Göttingen: Göttingen, Germany, 2016.